



# Experimental studies for the use of “beta enhancers” (BE) in the boron neutron capture therapy (BNCT) to optimize its application in the treatment of superficial tumors

Susana Isabel Nievas<sup>1</sup>, Marina Carpano<sup>2</sup>, Esteban Fabián Boggio<sup>3</sup>, Mariana Rosalia Casal<sup>1</sup>, Juan Manuel Longhino<sup>3</sup>, María Alejandra Dagrosa<sup>2,4</sup>

<sup>1</sup>Department of BNCT Coordination (CAC), National Atomic Energy Commission (CNEA), San Martín, Provincia de Buenos Aires, Argentina;

<sup>2</sup>Department of Radiobiology (CAC), National Atomic Energy Commission (CNEA), San Martín, Provincia de Buenos Aires, Argentina; <sup>3</sup>RA-6 (CAB), National Atomic Energy Commission (CNEA), Bariloche, Provincia de Río Negro, Argentina; <sup>4</sup>National Council of Scientific and Technical Research (CONICET), Ciudad Autónoma de Buenos Aires, Argentina

**Contributions:** (I) Conception and design: SI Nievas, EF Boggio, JM Longhino, MA Dagrosa; (II) Administrative support: JM Longhino, MA Dagrosa; (III) Provision of study material or patients: SI Nievas, M Carpano, EF Boggio; (IV) Collection and assembly of data: SI Nievas, M Carpano, MR Casal, EF Boggio, JM Longhino, MA Dagrosa; (V) Data analysis and interpretation: SI Nievas, EF Boggio, MR Casal, JM Longhino, MA Dagrosa; (VI) Manuscript writing: All authors; (VII) Final approval of manuscript: All authors.

**Correspondence to:** María Alejandra Dagrosa, PhD. Radiobiology Department (CAC), National Atomic Energy Commission (CNEA), Avenida General Paz 1499, (B1650KNA) San Martín, Provincia Buenos Aires, Argentina. Email: alejandradagrosa@gmail.com or dagrosa@cnea.gov.ar.

**Background:** Boron neutron capture therapy (BNCT) is based on the nuclear reaction  $^{10}\text{B} (n, \alpha) ^7\text{Li}$ . Due to the characteristics of the neutron beam (RA6), the maximum dose is 1 cm deep. Rhodium, indium and silver have a high effective neutron capture section, rapid decay activation products and high energy beta particles emission. Devices of these elements called beta enhancers (BE) can be used to compensate for the BNCT surface dose gradient or even to significantly increase it. In these experimental *in vivo* studies, we analyzed the therapeutic efficacy of rhodium, silver and indium BEs, and the advantages of adding them in BNCT to treat superficial tumors.

**Methods:** NIH nude mice were implanted subcutaneously with human colon cancer cells (HT 29), developing superficial tumors on day 15. Two irradiations of 37 and 45 minutes (Irradiation #1 and #2) with a thermal neutron flux of  $4.96 \times 10^8 \text{ n/cm}^2 \text{ sec}$  were performed. Boronophenylalanine was administered at 350 mg/kg (ip) and BEs of Rh, Ag and In, were placed on each tumor (Control, BNCT, BNCT Rh, BNCT Ag and BNCT In groups). The follow-up of mice was carried out for around 1 month.

**Results:** BE did not show any signs of radiotoxicity. Tumor growth decreased in all the groups treated by BNCT ( $P < 0.01$ ), in both irradiations (#1 and #2), rhodium BEs showed more effectivity than Ag and In BEs. Histological studies showed necrosis and a high presence of vacuoles and pycnotic nuclei in viable areas for the BNCT groups. Lower amounts of mitotic cells and CD133<sup>+</sup> cancer stem cells (CSCs) were observed in BNCT-Rh groups on days 7 and 23 in agreement with the tumor response and the absorbed physical dose.

**Conclusions:** A strong tendency to improve the therapeutic efficacy was observed in the BNCT-Rh group. However, these studies did not show significant differences among the three BEs evaluated with respect to BNCT alone. Besides, at the histological level, the rhodium element showed to induce greater cellular damage in the different subpopulations of tumor cells. Higher physical doses and boron-10 enriched compounds directed to CD133<sup>+</sup> CSC seem to be necessary to eliminate the presence of CSCs.

**Keywords:** Boron neutron capture therapy (BNCT); beta enhancers (BE); rhodium; indium; silver

Received: 22 August 2021; Accepted: 01 April 2022; Published: 30 June 2022.

doi: 10.21037/tro-21-24

View this article at: <https://dx.doi.org/10.21037/tro-21-24>

## Introduction

Boron neutron capture therapy (BNCT) is considered a radiotherapeutic modality based on the selective uptake of boron-10 enriched compounds by tumor tissues compared to surrounding normal tissues. Once the concentration of boron is optimum, the tumor area is irradiated with a thermal neutron beam.  $^{10}\text{B}$  turns into highly excited  $^{11}\text{B}$ , which immediately decays and releases an alpha particle and a  $^7\text{Li}$  nucleus. These particles of high-linear energy transfer (LET) are lethal for the boron-containing cells (1). BNCT is an alternative for some solid and localized tumors that do not respond to conventional therapies.

The Argentine clinical facility is located at the RA-6 Research Reactor in the Bariloche Atomic Center available for phase I–II malignant melanoma trials (2). The facility has a neutron beam designed for BNCT on superficial tumors that is called “hyperthermal”. This was developed through epithermal neutrons spectra moderation, including a partial thermalization stage in the beam, such as to provide a slow neutron flux maximum at approximately 1 cm depth in the irradiated tissue. Due to the penetration of the beam, the total absorbed dose in the first few millimeters of tissue is lower than in the maximum flux. Thus, the introduction of a suitable device over the irradiated volume has been considered to allow a local dose to increase without substantially perturbing the primary in-depth dose profile (original BNCT treatment). Some materials for the suggested devices such as rhodium, silver and indium have advantageous properties: a high neutron capture cross-section with fast decay activation products and high energy beta particles emission. As beta radiation has a short penetration range in tissue, it can be used to compensate the superficial dose gradient of the BNCT treatment, or even increase it significantly. Considering that such particles do not discriminate normal from tumor tissues, beta radiation-based devices are thought to be positioned on the anatomy surface, in a suitable configuration as close as possible to the target volume. These beta sources are called beta enhancers (BE) and make the most of backscattered thermal neutrons from the surface to a useful local dose contribution (3).

In the last years, the general conception of cancer has been changing. Evidences confirm that solid tumors have a complex cellular distribution with cells capable of generating blood vessels, cells with different proliferative capacity or different drugs resistance. Some of them are responsible of keeping the tumor alive, being the most important the cancer stem cells (CSCs) (4). CSCs can divide

and renew themselves and are resistant to chemo (5) and radiotherapy (6) and become recurrent or metastatic tumors; therefore controlling the proliferation of CSC is critical. It was proposed that CD133 could be a good surface biomarker of potential tumor stem cells (7). Also known as prominine-1 or AC133, CD133 is a 120-kDa transmembrane protein located primarily at the level of plasma membrane bumps. Furthermore, CD133, among other applications, could have clinical functions in predicting pathological stages, cancer recurrence, resistance to therapy, and survival of patients with colorectal carcinoma or melanoma (8,9).

At the Radiobiology Department, experimental studies of BNCT for cutaneous melanoma and other tumors superficially implanted in the nude mice, were performed to support clinical trials (10,11). The aim of these experimental studies was to evaluate the use of different materials (rhodium, silver and indium) BEs as a complementary tool in the application of BNCT to the treatment of superficial tumors and to analyze the presence and persistence of CSCs after the treatment. We present the following article in accordance with the ARRIVE reporting checklist (available at <https://tro.amegroups.com/article/view/10.21037/tro-21-24/rc>).

## Methods

### *Cell line*

The human HT-29 colon cancer cell line coming from a colorectal adenocarcinoma isolated from a 44-year-old patient (12), was kindly provided by Drs. G. Juillard, UCLA and J. Fagin, Cincinnati, USA). This cell line was maintained in RPMI 1640 culture medium supplemented with 154 mg/L of sodium pyruvate, 1.5 g/L of sodium bicarbonate, with 10% fetal bovine serum (FBS), streptomycin (100 mg/mL) and penicillin (100 UI/mL), at 37 °C in an atmosphere of 5% CO<sub>2</sub> and humidity at saturation. The study was conducted in accordance with the Declaration of Helsinki (as revised in 2013).

### *Animal model*

NIH nude mice (body weight 20–25 g) were implanted subcutaneously in the right back flank with 10<sup>6</sup> cells of the human (HT29) cell line. Animals were housed in covered cages and kept under aseptic conditions. After 15 days, when the tumors had a size between 50 and 100 mm<sup>3</sup>, the mice were

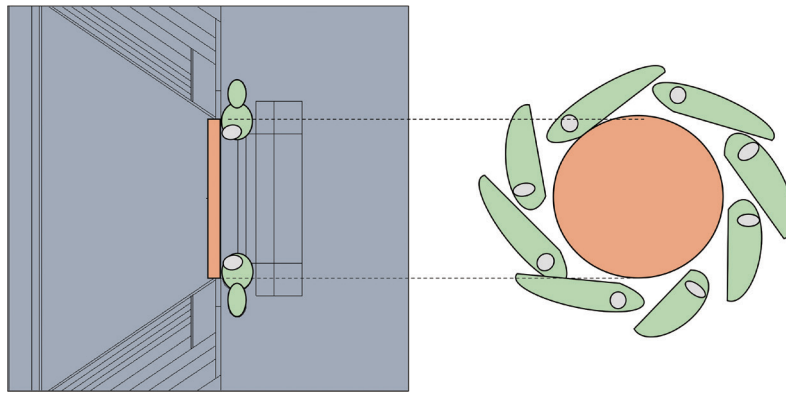


**Figure 1** Experimental setup for irradiation of small animals. Left: cone and neutron reflector protrude above the beam axis and small animals positioned around the neutron reflector.

used for the irradiation studies. Experiments were performed under a project license (Protocol N°6/2018 Studies of alternative therapies for the treatment of the cancer) granted by the Argentine National Atomic Energy Commission Animal Care and Use Committee (CICUAL-CNEA) in compliance with the National Institute of Health (NIH USA) guide for the care and use of laboratory animals (13).

### ***Boron solution preparation***

The stock solution of boronophenylalanine  $^{10}\text{BPA}$ -fructose was prepared at a concentration of 30 mg  $^{10}\text{BPA}$  per mL (0.14 M).  $^{10}\text{BPA}$  (99%  $^{10}\text{B}$  enriched, L-isomer) (Interpharma Praha S.A., Czech Republic) was combined in water with a 10% molar excess of fructose. The pH was adjusted to 9.5–10 with sodium hydroxide (NaOH), and the mixture was stirred until all solids dissolved. Afterward, pH was readjusted to 7.4 with hydrochloric acid (HCl) (14).

### ***Experimental design and irradiation setup***

Two experiments of irradiation were performed on different dates after the modifications in the Argentine clinical facility (Irradiations #1 and #2). In both studies, the animals were irradiated in the RA6 reactor beam (Neutron flux at tumor position:  $4.96 \times 10^8$  n/cm<sup>2</sup> sec). The irradiation setup at the beam is shown in *Figure 1*. In order to adapt the clinical BNCT beam to small animal irradiations, the protruding cone is supplemented with a central neutron reflector. Groups of 8 animals on a mobile plate were irradiated for 37 minutes (Irradiation #1) and 45 minutes (Irradiation #2). The (0.14 M) boronophenylalanine (BPA) solution was

administered to the animals at a dose of 350 mg/kg b.w via intraperitoneal (ip).

Before the treatment, the mice were anesthetized with a combination of diazepam (40 mg/kg) and ketamine (200 mg/kg), both subcutaneously administered, with a lapse of 20 minutes between them. Over the tumor, a foil BE with the diameter corresponding to each tumor size was placed with hypoallergenic tape (*Figure S1*). The BE materials used in this study were obtained from standard Neutron Activation materials used in the RA6 reactor for neutron physics experiments. As such, these high-purity materials (99.99%) are in foil format, with thicknesses related to that use. The thicknesses of the foils were: 0.025 mm for rhodium and 0.127 mm for silver and indium.

The neutron irradiation was performed at the moment of maximum boron concentration in tumor. These studies were based on previous boron biodistributions results (15). *Table 1* describes the main radiochemical characteristics of the BEs materials used in different groups of animals and *Table 2* describes the products of neutron capture reaction in rhodium, silver and indium (16–19).

### **Irradiation #1**

Nude mice were separated into five groups of 6–8 animals each: (I) Control group: without boron compound and not irradiated (n=7); (II) neutron capture therapy (NCT): without boron compound and irradiated with neutron beam alone (n=6); (III) NCT-Rh: without boron compound and irradiated with neutron beam alone plus BE rhodium (n=7); (IV) BNCT: BPA and irradiated with neutron beam (n=7); (V) BNCT-Rh: BPA plus BE rhodium and irradiated with neutron beam (n=8).

**Table 1** Beta enhancers nuclear properties

Radiochemical characteristics	Rhodium	Silver	Indium
Isotope of interest	Rh-109	Ag-107/Ag-109	In-115
Abundance (%)	100	52/48	96
Thermal cross section (b)	143	38/91	201
Resonance integral (b)	969	107/1,474	3,210
Max. beta energy (keV)	2,448	1,654/2,892	3,276/1,137
Half-live (min)	0.7	2.4/0.4	0.2/54
Beta decay yield (%)	100	97/100	21/79

The main radiochemical characteristics of the BEs are listed. The thicknesses used in these studies were: rhodium: 0.025 mm; silver and indium: 0.127 mm. BE, beta enhancers.

**Table 2** Energy of beta and gamma radiation of BE

Rhodium			Silver			Indium		
Beta (-) radiation		Gamma radiation	Beta (-) radiation		Gamma radiation	Beta (-) radiation		Gamma radiation
Maximum energy (Mev)	Most likely energy (Mev)	Energy (Mev)	Maximum energy (Mev)	Most likely energy (Mev)	Energy (Mev)	Maximum energy (Mev)	Most likely energy (Mev)	Energy (Mev)
2.5 (98%)	1.0	0.5 (2%)	2.9 (100%)	1.2	0.9 (75%)	3.3 (98%)	1.4	1.3 (85%)
1.9 (1.9%)	0.7	0.8 (<0.1%)	1.7 (95%)	0.6	0.9 (35%)	2.0 (100%)	0.8	1.1 (56%)
1.2 (<0.1%)	0.5	1.2 (<0.1%)			1.4 (25%)	1.0 (54%)	0.4	2.1 (15%)
					1.5 (13%)	0.9 (32%)	0.3	1.5 (10%)
						0.6 (10%)	0.2	0.9 (12%)
								1.75 (2%)

Distribution of energies beta y gamma for each BE used (rhodium, silver and indium). BE, beta enhancers.

## Irradiation #2

Nude mice were separated into five groups of 5–8 animals each: (I) Control: without boron compound and not irradiated (n=8); (II) BNCT: BPA and irradiated with neutron beam (n=6); (III) BNCT-Rh: BPA plus BE rhodium and irradiated with neutron beam (n=5); (IV) BNCT-Ag: BPA plus BE silver and irradiated with neutron beam (n=6); (V) BNCT-In: BPA plus BE indium and irradiated with neutron beam (n=7).

## Dosimetric evaluation

*In vivo* measurements were performed during irradiation, as well as in mice phantoms replicating the actual positioning. In all cases, detectors for neutron flux and photon beam were selected in order to minimize experimental perturbation. All

reported doses correspond to physical doses.

Suitable detectors were placed at several external and internal positions of the phantoms (equivalent to the actual tumor position, and in positions correspondent to abdomen, torso, and head), as well as in superficial contact with the actual mouse. As a complement to the experimental measurements, dosimetric parameters (perturbations, cross section, flux-to-dose conversions, relative geometric distributions, etc.) were obtained using the MCNP5 model of the facility including the experimental setup.

The photon dose rate was measured using TLD-700 (Harshaw) (3.2×3.2×0.9 mm<sup>3</sup>). The estimation of the fast neutrons flux was performed using the threshold inelastic reaction of the <sup>115</sup>In isotope in a pure indium massive foil (2 mm thick, 20 mm in diameter and approximately 4.5 g). Thermal neutron fluxes (neutron energies below 0.5 eV)

were determined by measurements with activation detectors whose cross sections are similar to those of Nitrogen and Boron (approximately 1/v), such as manganese or copper.

$^{14}\text{N}$  and  $^{10}\text{B}$  dose rates were obtained from tissue thermal neutron Kerma factor and the measured thermal flux in each position. The concentration of  $^{10}\text{B}$  was assumed to be 21 ppm in the tumor, while in the surrounding skin was 12.5 ppm (15). As for  $^{14}\text{N}$ , it is assumed to be 2.8% in each body part. Fast neutron doses were also correspondingly obtained by means of measured fast flux; a conversion factor condensed from the neutron Kerma factors and the calculated neutron spectra in the Indium irradiation position.

Beta enhancer doses were evaluated indirectly for both skin (external, superficial tissue 0.5 mm thick layer) and tumor (internal, averaged for 1 to 5 mm tumor diameter). The relative contribution was obtained from MCNP5 calculation, while the dose-to-flux scaling factor was obtained for the asymptotic activation condition from a specific experiment. Total absorbed physical dose for each mice group was calculated by adding each dose rate components (fast neutrons, photon and thermal neutrons, BE dose when corresponding) and multiplying by the irradiation time.

### *Follow up studies*

Radiotoxicity and tumor growth in animals were monitored for around 1 month post treatment. After the first and the third weeks (days 7 and 23), several animals from each group were sacrificed and histological and immunohistochemical studies were performed.

### **Radiotoxicity**

Short-term toxicity of each BE was evaluated through control of body weight and the appearance of visible skin injuries.

### **Tumor growth**

The tumor size was measured with a caliper twice a week and the volume was calculated according to the following formula:

$$\text{Tumor volume} = (A^2 \times B) \div 2 \quad [1]$$

Where A is the width and B is the length (20).

### **Hematoxylin and eosin (HE) stains and immunohistochemistry**

Histological preparations from the tumor and the

surrounding skin were performed at the first and third week after irradiation. Briefly, tissues were fixed with 10% buffered formaldehyde (pH 7.0) and paraffin embedded. Ten-micron-thick sections were cut and stained with HE. All sections for immunohistochemistry were deparaffinized and rehydrated using graded concentrations of ethanol prepared with deionized water. The slides were transferred into a 0.05 M Tris-based solution in 0.15 M sodium chloride (NaCl) with 0.1% v/v Triton-X-100, pH 7.6 (TBST). Endogenous peroxidase was blocked with 3% hydrogen peroxide for 10 min. Antigen retrieval was done using microwave in citrate buffer at pH 6.0. All slides were incubated at room temperature for 1 h with one antibody: monoclonal mouse anti CD133 human (Miltenyi Biotec, N° 130-090-422). Using a kidney and liver sections as controls, the highest titer of primary antibodies to produce optimal demonstration of micro vessels with the lowest acceptable background staining was 1:50 for CD133 human (Miltenyi Biotec, N° 130-090-422). Negative controls were produced by eliminating the primary antibody from the diluents. After washing with phosphate buffer saline (PBS)-Tween, biotinylated goat anti-mouse IgG (1:1,000; Cell Marque) was applied to the sections for 30 minutes at room temperature. Sections were then incubated with Streptavidin-HRP (Sigma) for 30 minutes at room temperature. Diaminobenzidine (DAB) was used as the chromogen and hematoxylin as the counterstain. Sections were mounted for examination. Stained slides were imaged at 0.25  $\mu\text{m}$  per pixel resolution using a ScanScope XT. The Image Pro Plus program was used to analyze the intensity of antibody labeling.

A rectangular band was scanned in a histological section, taking consecutive images, covering the central area of each histological section of approximately 300  $\mu\text{m}$   $\times$  6,400  $\mu\text{m}$ , which includes all the tumor growth. On the other hand, it is an adequate indicator of the relationship of biochemical data with the real values of viable tissue, tissue in regeneration and areas of cell death. Through an imaging program (IMAGE-PRO PLUS Version 6.0), percentages of viable area and necrotic area, numbers of mitotic cells were evaluated.

### *Statistical analysis*

All results are expressed as the average of 5–8 samples  $\pm$  standard error (SE). For statistical analysis of tumor growth, studies one-way ANOVA followed by a post-hoc test were performed using the Bonferroni test to make a multiple

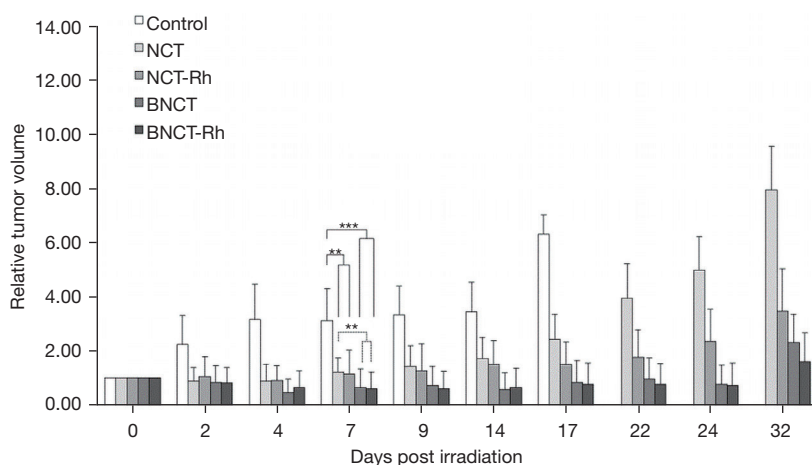


**Figure 2** Tumor growth after Irradiation #1. Relative tumor volume as a function of the time post irradiation in days, for each mice group (Control; NCT; NCT-Rh, BNCT and BNCT-Rh). Each point value is the mean  $\pm$  SE of 6–8 animals. At day 7: \*\*,  $P < 0.01$  for NCT and NCT-Rh *vs.* Control, BNCT and BNCT-Rh *vs.* NCT; \*\*\*,  $P < 0.001$  for BNCT and BNCT-Rh *vs.* Control. NCT, neutron capture therapy; Rh, rhodium; BNCT, boron neutron capture therapy.

comparison. Differences were considered significant when  $P < 0.05$ .

## Results

### Irradiation #1

Post-irradiations monitoring did not evidence any sign of toxicity in the treatment tumor volume with the BE rhodium. Relative tumor volume as a function of the time for each mice group are indicated in *Figure 2*. It can be observed that tumor growth was controlled until day 15 for both NCT groups and until day 25 approximately for both BNCT groups, and then re-starts growing (The significance level on day 7 was: \*\* $P < 0.01$  for NCT and NCT-Rh *vs.* Control; BNCT and BNCT-Rh *vs.* NCT; \*\*\* $P < 0.001$  for BNCT and BNCT-Rh *vs.* Control).

A considerably improvement was observed in the NCT-Rh and BNCT-Rh groups respect to the NCT and BNCT groups respectively. These results showed the first evidence of therapeutic contribution of the BE.

Histological studies did not show differences in the percentage of viable tissue between the different treatments, neither at one week nor three weeks after irradiation (*Figure 3*). However, the immunohistochemical studies carried out in these tumor samples to determine the presence and amount of potential CSC through the membrane marker CD133 showed that the BNCT-Rh

group had a lower number of CD133 positive CSCs in the viable area at three weeks (*Figure 4A-4D*).

### Irradiation #2

In this study we added BNCT groups with BE of other materials (rhodium, silver and indium). The evaluation of the body weight in the animals, as an indicator of radiotoxicity, did not show significant variations over time for any group (*Figure 5*). Regarding of skin radiotoxicity, only mild erythema was observed in the tumor area and skin surrounding the tumor in the BNCT-In group. The cutaneous injury lasted during the first days after irradiation (initial phase of erythema), and then reversed completely.

In the *Figure 6* the relative tumor volume as a function of the days post irradiation is graphed. In this figure, a partial remission or a tumor growth inhibition can be observed, in all the BNCT groups compared to the Control group (at day 7:  $P < 0.05$  for BNCT-Rh *vs.* Control. At day 23:  $P < 0.01$  for BNCT-Ag *vs.* Control and  $P < 0.001$  for BNCT, BNCT-Rh and BNCT-In *vs.* Control). However, it is important to point the decrease in the tumor growth in the BNCT-Rh group throughout the evaluation period compared to the other groups. Although the difference between irradiated groups was not statistically significant, it is important to point the decrease in the tumor growth in the BNCT-Rh group through out the evaluation period compared to the other groups.

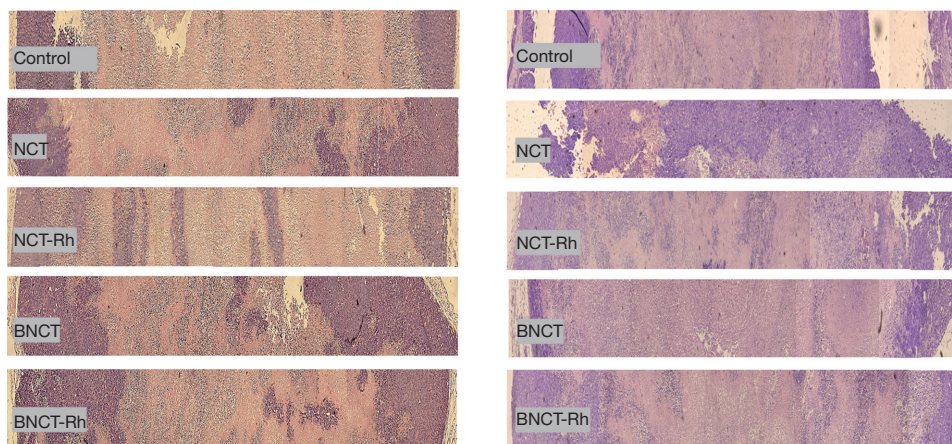


**Figure 3** Histological analysis for tumor samples of the different treatments (Control, NCT, NCT-Rh, BNCT, BNCT-Rh) after Irradiation #1. Histological sections with HE stains, magnification 20 $\times$ . Left: day 7. Right: day 23. Percentages of viable areas were measured and compared between animals of the different treatments. NCT, neutron capture therapy; Rh, rhodium; BNCT, boron neutron capture therapy; HE, hematoxylin and eosin.

The histological studies at 7 days post-irradiation, showed in all the BNCT treatments an important percentage of necrosis. In viable areas the important presence of vacuoles, pyknotic nuclei and mitotic cells can be observed (*Figure 7A*). The high presence of vacuoles can be related to the cell death by autophagy process (21). In the zone of viability, a lower number of mitotic cells in the BNCT-Rh group, was observed (*Figure 7B*). *Figure 8A-8C* shows the results of immunohistochemical studies about CD133 positive CSCs in viable areas. *Figure 8A,8B* shows the percentage of viability and the number of CD133 positive CSC for each treatment respectively. A better response for BNCT and BNCT-Rh groups than in the other treatments can be observed. But when the relationship between CD133<sup>+</sup> CSC and viability was analyzed, an improvement for BNCT-Rh group was observed. These results indicate the survival of CSC at three weeks. Although the amount of CSC was lower than the rest of the groups, it could reveal the reason for the observed tumor regrowth.

### Dosimetric calculation

The dosimetric results showed a higher total absorbed physical dose for all the treatments in the second irradiation (Irradiation #2) compared to the first irradiation (Irradiation #1). The increase was due to the longer irradiation time. The neutron fluence was effectively larger.

*Tables 3,4* show the results of the dosimetric calculations. The BNCT total absorbed physical doses to tumor were

4.83 and 5.74 Gy for the first and the second irradiation respectively. With the use of BE rhodium the total absorbed physical dose incremented in the tumor 1.14 and 1.36 Gy respectively (BNCT-Rh for Irradiation #1 and #2).

The addition of the BE devices over the skin atop the tumor added to the total absorbed physical dose, other components (gamma and beta radiation), whilst minimally perturbing the straight away dosimetry of the original BNCT treatment. The compounded total physical absorbed dose, including the radiation released by silver and indium during the second irradiation were respectively 8.00 and 6.55 Gy at the tumor (*Table 4*). This represents an increase of 2.26 Gy for BNCT-Ag and 0.81 Gy for BNCT-In, respect to BNCT alone. The comparison of the three BE showed a higher increase in the total dose for the silver. The results of dosimetry showed in this work, indicated that this increase was not reflected in biological damage indicators analyzed here.

As the BE was selected as a source of secondary radiation under neutron irradiation (and specifically beta minus radiation), the local increase of absorbed physical dose is higher the closer the tissue is relative to the BE emitter. Thus, skin tissue under BE, receives a dose boost higher than the rest of the tumor. This trend is especially noticeable for Rh and Ag. It is also to be expected a similar differential dose deposition of the component due to the BE influence (when present) inside the tumor volume, albeit such distribution was not considered in the present work (*Figure S2*).

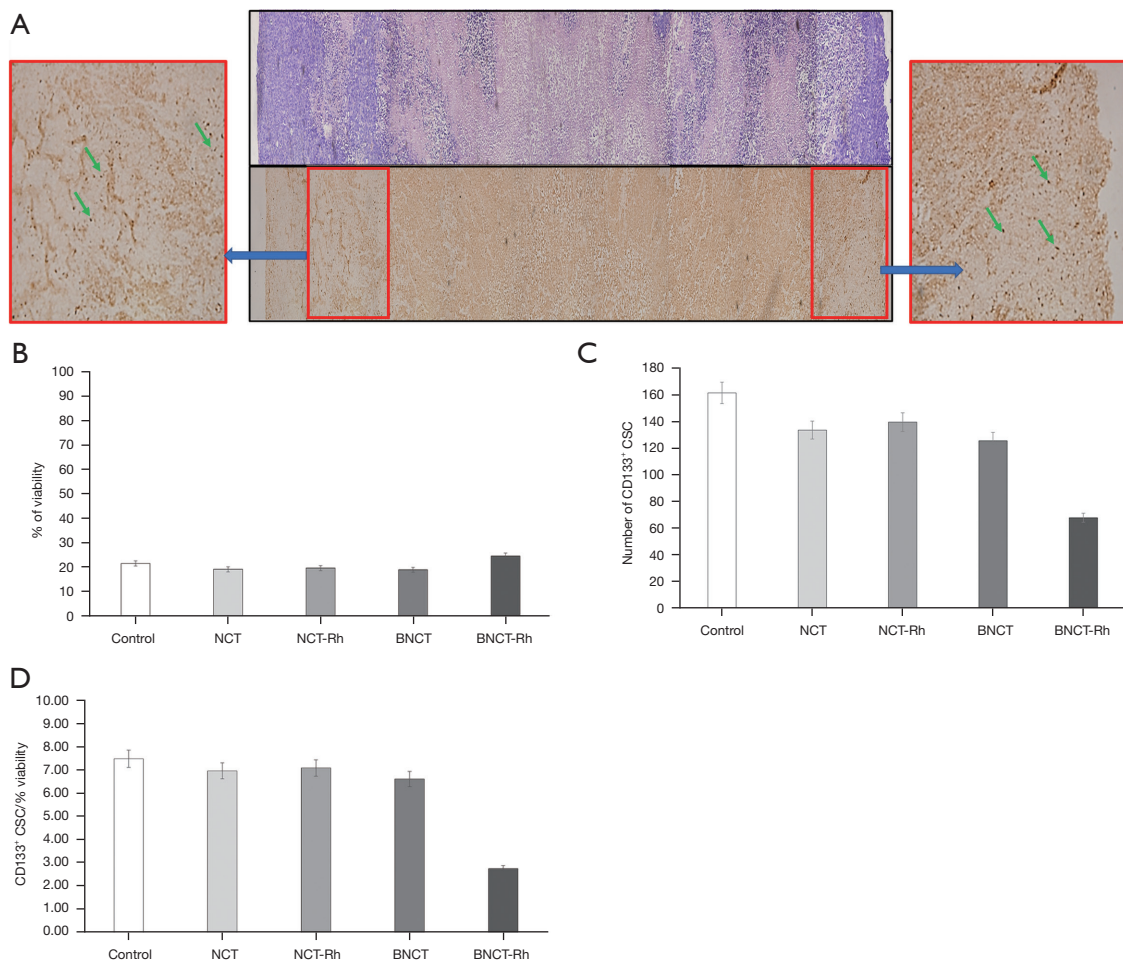


**Figure 4** Histological and immunohistochemical studies for tumors (Irradiation #1) (A-D). (A) Representative micrographs of same tumoral tissue sample of BNCT-Rh stained with HE (up) and immunohistochemical for CD133 antibody (down) at day 23. Magnification 20 $\times$ . Insets show magnified view of the viable area with green arrows pointing out CD133<sup>+</sup> CSC. (B-D) The % of viability, the amounts of CD133<sup>+</sup> CSC (C) and the relationship of CD133<sup>+</sup> CSC and % viability (D) at 23 days for each treatment (Control, NCT, NCT-Rh, BNCT and BNCT-Rh) are shown. CSC, cancer stem cell; NCT, neutron capture therapy; BNCT, boron neutron capture therapy; HE, hematoxylin and eosin.

In all measurements, deviations of the external thermal flux of approximately 10% (minimum 6% in phantoms, average 19% in phantoms and 19% in total *in vivo*) are observed. The internal thermal flux is 27% higher than the external thermal flux. There is no evidence of greater differences in the flux by the BE.

## Discussion

These studies were carried out in order to support clinical studies in the new beam of RA-6 (Argentine Bariloche Atomic Center). Our main objective was to evaluate the

use of beta enhancer devices of different materials as a complementary tool to BNCT. On the other hand, and in order to evaluate therapeutic efficacy, the presence and persistence of potential CSCs through CD133 surface biomarker was analyzed.

In our first studies, we showed that nude mice bearing superficial tumors and irradiated by BNCT with the addition of rhodium as BE, did not show signs of radiotoxicity. We also showed an enhancement in the control of the tumor growth irradiated under rhodium BE. In addition, the histological studies revealed greater tumor damage and the immunohistochemical analysis

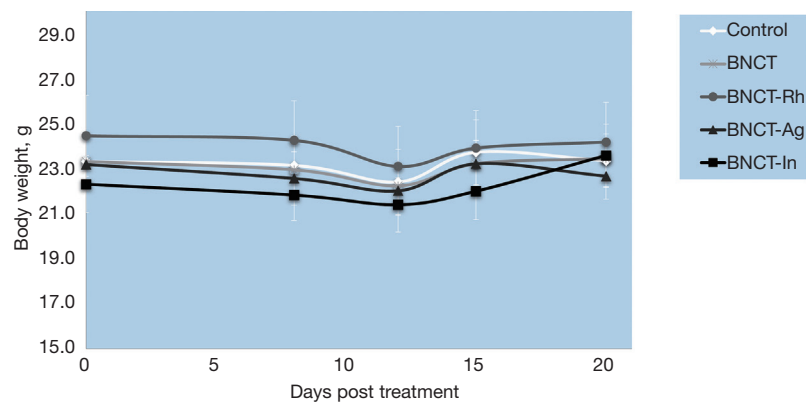


**Figure 5** Body weight as a function of the days post treatments (Control, BNCT, BNCT-Rh, BNCT-Ag, BNCT-In). No significative differences were observed. BNCT, boron neutron capture therapy.

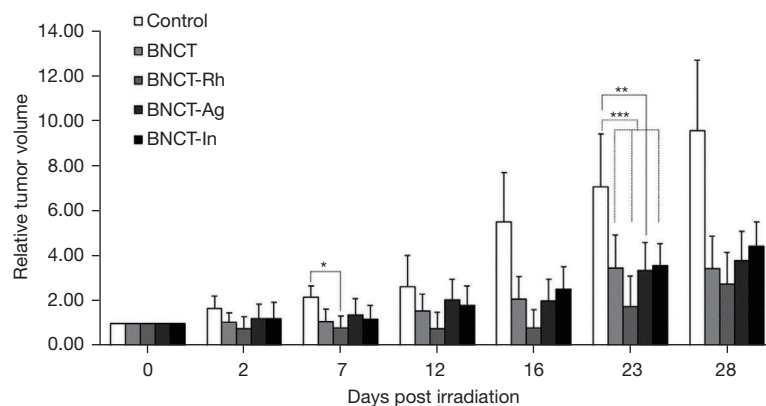


**Figure 6** Tumor growth after Irradiation #2. Relative tumor volume as a function of the time post irradiation in days, for each mice group (Control, BNCT, BNCT-Rh, BNCT-Ag, BNCT-In). Each point value is the mean  $\pm$  SE of 5–8 animals. At day 7: \*,  $P < 0.05$  for BNCT-Rh vs. Control; At day 23: \*\*,  $P < 0.01$  for BNCT-Ag vs. Control; \*\*\*,  $P < 0.001$  for BNCT, BNCT Rh and BNCT-In vs. Control. BNCT, boron neutron capture therapy.

showed a lower number of CD133 positive CSC at 23 day for BNCT-Rh. As a continuation of these studies with encouraging results, other emitting devices of beta radiation (silver and indium) began to be evaluated. The comparison between the different materials allowed to make the most appropriate selection of BE.

As an indicator of radio toxicity the body weight of the animals was monitored during the follow-up time in addition to the macroscopic observation of the tumor area and the surrounding skin. Regarding body weight, no significant differences were observed between the animals of all the groups. In the BNCT group with indium devices, a slight erythema was observed in the skin surrounding the tumor during the first days after treatment. This

erythema reverted after a week and its development agrees with the characteristics described for the initial phase in the evolution of a radiation-induced erythema, presented in the Radiological Protection Guide for Patients of the International Atomic Energy Agency (IAEA) (22). We tried to find a relationship between the injury and the main radiochemical characteristics of each material. We found that, in the case of indium BE a higher 54 minutes decay mode comes into play as the irradiations were longer. This mode has four low energy beta emissions, as well as a number of gamma photons, making this case more “impure” in comparison with rhodium or silver. Thus the absorbed dose with indium is relatively more deposited on the tumor surface than in the case of rhodium and silver. The graph of

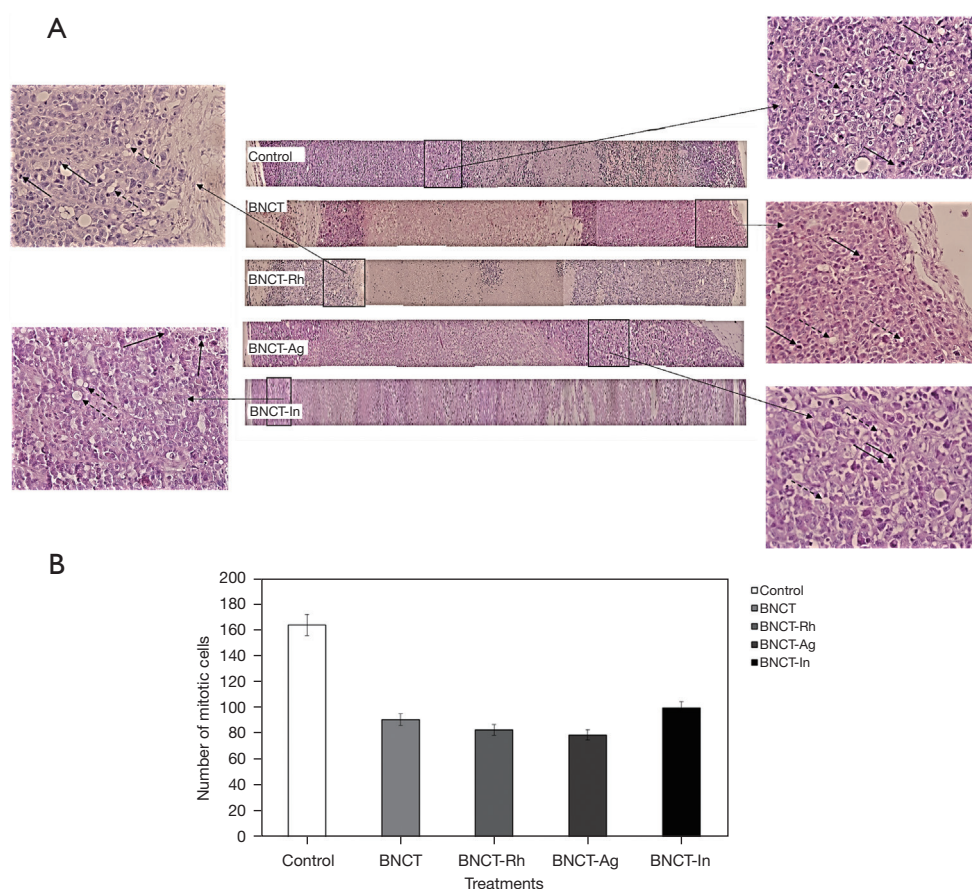


**Figure 7** Histological analysis of a rectangular portion running through the entire tumor at day 7 for the different groups (Irradiation #2). (A) Histological sections with HE stains, magnification 20x. Insets show magnified view of the viable area with a high presence of vacuoles (black arrows with dotted lines) and mitotic cells (black arrows with whole lines). (B) Histogram showing the amounts of mitotic cells for each group. BNCT, boron neutron capture therapy.

relative tumor volume as a function of time post treatment for Irradiation #2 showed that the tumor stopped its growth after irradiation until the third week, in the four BNCT groups. This decrease in tumor volume of the all the BNCT groups with respect to the non-irradiated group (Control) was significant  $P < 0.01$ , although it was not significant between the irradiated groups only. Despite statistical results did not show an improvement of any BE over BNCT alone, we observed a better qualitative response for the BNCT-Rh group. One reason to explain the superiority of rhodium could be related to its high ratio of electrons of high-energy generated per unit mass of BE. For the same reason, also it would end up disturbing the neutron beam less and self-attenuating the generated electrons themselves.

From day 20, all animals showed a loss of inhibition on tumor growth. This second irradiation agrees with previous

results obtained by our group applying BNCT without the addition of the BE device for superficial tumors greater than  $50 \text{ mm}^3$  (23). A behavior of this type was described in the literature for tumors irradiated with suboptimal doses of conventional radiation.

In this work, histological studies of the tumor samples showed a lower percentage of the viable area in the treated groups compared to the Control group. The analysis of mitotic cells showed that the number of cells that are dividing is lower than in the four treatments and more important the decrease in the BNCT Rh group. Other studies demonstrated an arrest in G2/M and defects in the mitosis of different cancer cell lines after BNCT treatment (24-27). Our results would confirm the arrest in this phase of the cell cycle after exposing tumor cells in culture at total physical doses of 3 Gy from BNCT (28).

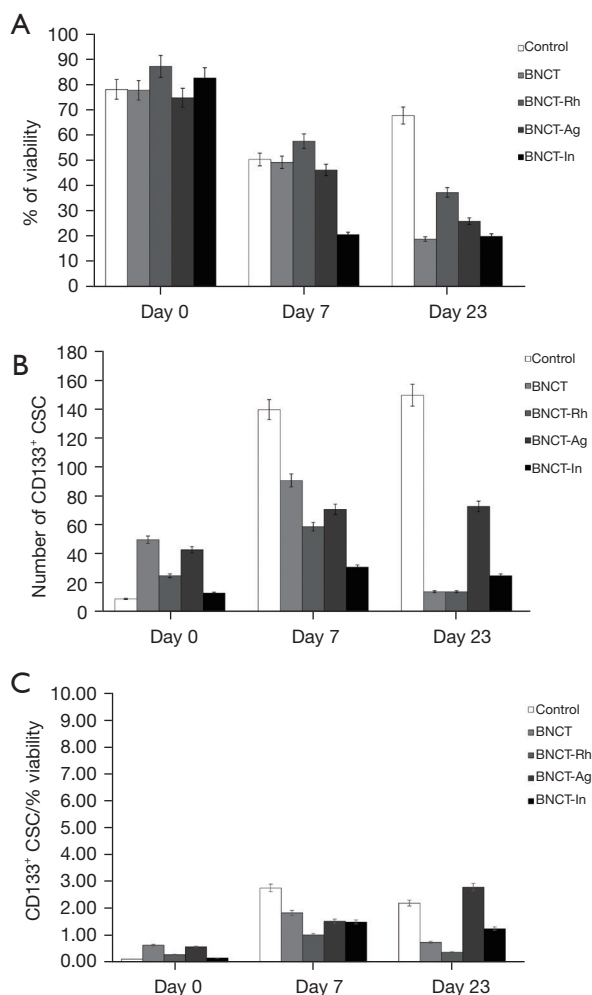


**Figure 8** The % of viability (A), the amounts of CD133 positive CSC (B) and the relationship between CD133<sup>+</sup> CSC and viability for each group (C) are shown. BNCT, boron neutron capture therapy; CSC, cancer stem cell.

Also these histological tumor samples showed a high presence pyknotic nuclei and vacuoles in the viable areas for BNCT-BE treatments. The finding of increased vacuoles could be related with the autophagy as mechanism of death. The main mechanism of cell death produced by high-LET radiation (such as that from BNCT) that have been described in the literature is mitotic catastrophe or tissue necrosis. Also apoptosis is indicated as another probable and secondary pathway of radio-induced death. A third biological process of cell death would be autophagy, which was described as a catabolic process of degradation in response to different types of stress (29). Other studies showed that in cells with the over-expressed antiapoptotic Bcl XL gene, death is induced by autophagy (21). Our results would agree with these three mechanisms and in the same proportion indicated, although the greater number of vacuoles observed for the BNCT-BE group could indicate an increase in autophagy probably associated with the additional low LET absorbed dose of the beta radiation contribution. Experimental and calculation studies demonstrate that all the BE considerable contributed to the total absorbed dose, but rhodium is the one that almost non-perturb the BNCT beam (3).

CD133 positive cells indicated the presence of potential CSCs in the viable area of the tumor generated in nude mice by the implantation of cells of the HT-29 human carcinoma cell line. Its persistence, although diminished, one (Irradiation #2) and three weeks (Irradiation #1) after irradiation, would seem to be associated with tumor proliferation and loss of control over the growth of therapy with any of the devices used. Oncology studies showed that these CSCs are the most radioresistant cells and they should be the target of any therapy that is implemented since they

**Table 3** Dosimetry for Irradiations #1 and #2

Irradiation	Irradiation time (min)	Thermal flux (n/cm <sup>2</sup> seg)	Absorbed physical dose (Gy) by the tumor					
			<sup>10</sup> B dose	<sup>14</sup> N dose	Photondose	Fast neutronsdose	Total NCT dose (w/o <sup>10</sup> B)	Total BNCT dose
#1	37	4.96×10 <sup>8</sup>	2.3	0.2	1.8	0.7	2.7	5.0
#2	45.3		2.5	0.3	2.2	0.8	3.3	5.8

Dose rate components obtained through the calculation model in MCNP5 for the tumor tissue for Irradiations #1 and #2. Total absorbed physical dose was calculated by the addition of all the component doses (photon, <sup>10</sup>B, <sup>14</sup>N, fast neutrons). The uncertainties of the total dose rates in tumor are around 3%. Uncertainties associated with the boron compound or nitrogen are not considered. NCT, neutron capture therapy; BNCT, boron neutron capture therapy.

**Table 4** Dosimetry of BNCT + beta enhancers for irradiations #1 and #2

Tissue	$\mu\text{g/g}$ of $^{10}\text{B}$	Total absorbed physical dose for all the treatment groups (Gy)							
		Irradiation #1				Irradiation #2			
		NCT	NCT-Rh	BNCT	BNCT-Rh	BNCT	BNCT-Rh	BNCT-Ag	BNCT-In
Tumor	21	2.7	3.8	5.0	5.8	5.7	9.1	9.9	7.0
Surrounding skin	12.5	2.7	5.4	3.9	6.6	4.7	8.1	8.9	6.0

Comparison of the total absorbed physical dose (Gy) between the different treatment groups (Gy) for both irradiations #1 and #2. Boron concentration for all the tissues were taken of previous BPA biodistribution (15). BNCT, boron neutron capture therapy; NCT, neutron capture therapy; BPA, boronophenylalanine.

have the properties to generate the tumor again (30). The total physical doses absorbed by the tumors were of 7.10 for BNCT-Rh, of 8.00 for BNCT-Ag and of 6.55 Gy for BNCT-In. At the macroscopic level, in agreement with these dose values, no significant differences in tumor growth were observed among the four treated groups, although it was observed a strong tendency to decrease for the BE-Rh. Also, at the microscopic level with the BE-Rh a greater biological effect was obtained in terms of a lower number of mitosis cells and lower number of CD133 positive CSCs at 7 and 23 days after irradiation.

Surface biomarkers are commonly used for the identification and isolation of CSCs. CD133, CD44 and CD24 are the three highest value markers proposed for colon cancer. Other authors have isolated CSC CD133 positive from the HT29 cell line and have evaluated their functional characteristics (self-renewal and tumorigenic and metastatic capacities) (31). Furthermore CD133 could have clinical functions in predicting pathological stages, cancer recurrence, resistance to therapy, and survival of patients with colorectal carcinoma (8). Current therapies exhibit cytotoxic effects that kills most of the tumor cells, but they are not fully effective, and some tumors reappear, sometimes with even greater pathogenicity. If the importance of stem cells in this reappearance is demonstrated, new therapies should specifically target CSCs in an attempt to impede CSC resistance and tumor regeneration. So far, there are little data that related BNCT therapy with CSCs, so the information obtained with our studies respect to CSCs will be useful to redirecting the boron therapy.

At cellular level, the rhodium element showed to induce greater cellular damage in the different subpopulations of tumor cells. About of the biosafety of this element, the rhodium is a precious metal, from the platinum family of metals, known to be bioinert. This one in particular is of low corrosivity, low cytotoxicity, moderate in mutagenic effects and allergies. On the other hand, rhodium is used

superficially, resting on the skin (32).

Higher doses of neutrons seem to be necessary to eliminate the presence of CSC. Another alternative would be targeting CD133 positive CSCs using boron-10 enriched compounds directed to this population. Following the same goal, Sun *et al.* (33) developed a bioconjugate nanoparticle that targets human CD133 positive glioma stem cells (GSCs) and would be a potential boron agent in BNCT. Later Kondo *et al.* (34) showed that glioma stem-cell like cells (GSLCs) may take up BPA and be amenable to targeting by BNCT.

## Conclusions

A strong tendency to improve the therapeutic efficacy was observed in the BNCT-Rh group. However, these studies did not show significant differences in the use of the three devices BE evaluated with respect to BNCT alone. Also, at the histological level, the rhodium element showed to induce greater cellular damage and a lower number of CD133 positive CSC. Higher physical doses and boron-10 enriched compounds directed to this population seem to be necessary to eliminate the presence of CSCs.

## Acknowledgments

*Funding:* The study was supported by National Commission of Atomic Center and grants from National Agency for Scientific and Technological Promotion and National Council of Scientific and Technical Research.

## Footnote

*Reporting Checklist:* The authors have completed the ARRIVE reporting checklist. Available at <https://tro.amegroups.com/article/view/10.21037/tro-21-24/rc>

*Conflicts of Interest:* All authors have completed the ICMJE

uniform disclosure form (available at <https://tro.amegroups.com/article/view/10.21037/tro-21-24/coif>). The authors have no conflicts of interest to declare.

**Ethical Statement:** The authors are accountable for all aspects of the work in ensuring that questions related to the accuracy or integrity of any part of the work are appropriately investigated and resolved. The study was conducted in accordance with the Declaration of Helsinki (as revised in 2013). Experiments were performed under a project license (Protocol N°6/20 “Studies of alternative therapies for the treatment of the cancer”) granted by the Argentine National Atomic Energy Commission Animal Care and Use Committee (CICUAL-CNEA) in compliance with the National Institute of Health (NIH USA) guide for the care and use of laboratory animals.

**Open Access Statement:** This is an Open Access article distributed in accordance with the Creative Commons Attribution-NonCommercial-NoDerivs 4.0 International License (CC BY-NC-ND 4.0), which permits the non-commercial replication and distribution of the article with the strict proviso that no changes or edits are made and the original work is properly cited (including links to both the formal publication through the relevant DOI and the license). See: <https://creativecommons.org/licenses/by-nc-nd/4.0/>.

## References

- Barth RF, Mi P, Yang W. Boron delivery agents for neutron capture therapy of cancer. *Cancer Commun (Lond)* 2018;38:35.
- Menéndez PR, Roth BM, Pereira MD, et al. BNCT for skin melanoma in extremities: updated Argentine clinical results. *Appl Radiat Isot* 2009;67:S50-3.
- Boggio E, Longhino J, Provenzano L, et al. Beta Enhancers: towards a local dose enhancer device for Boron Neutron Capture Therapy (BNCT) on superficial tumors. *IFMBE Proceedings. World Congress on Medical Physics and Biom* 2015;51:607-13.
- Al-Hajj M, Clarke MF. Self-renewal and solid tumor stem cells. *Oncogene* 2004;23:7274-82.
- Liu YS, Hsu HC, Tseng KC, et al. Lgr5 promotes cancer stemness and confers chemoresistance through ABCB1 in colorectal cancer. *Biomed Pharmacother* 2013;67:791-9.
- Krause M, Dubrovska A, Linge A, et al. Cancer stem cells: Radioresistance, prediction of radiotherapy outcome and specific targets for combined treatments. *Adv Drug Deliv Rev* 2017;109:63-73.
- O'Brien CA, Pollett A, Gallinger S, et al. A human colon cancer cell capable of initiating tumour growth in immunodeficient mice. *Nature* 2007;445:106-10.
- Wahab SMR, Islam F, Gopalan V, et al. The Identifications and Clinical Implications of Cancer Stem Cells in Colorectal Cancer. *Clin Colorectal Cancer* 2017;16:93-102.
- Madjd Z, Erfani E, Gheytanchi E, et al. Expression of CD133 cancer stem cell marker in melanoma: a systematic review and meta-analysis. *Int J Biol Markers* 2016;31:e118-25.
- Carpano M, Perona M, Rodriguez C, et al. Experimental Studies of Boronophenylalanine ((10)BPA) Biodistribution for the Individual Application of Boron Neutron Capture Therapy (BNCT) for Malignant Melanoma Treatment. *Int J Radiat Oncol Biol Phys* 2015;93:344-52.
- Perona M, Majdalani ME, Rodríguez C, et al. Experimental studies of boron neutron capture therapy (BNCT) using histone deacetylase inhibitor (HDACI) sodium butyrate, as a complementary drug for the treatment of poorly differentiated thyroid cancer (PDTTC). *Appl Radiat Isot* 2020;164:109297.
- Fogh J, Trempe G. New Human Tumor Cell Lines. In: Fogh J. editor. *Human Tumor Cells in Vitro*. New York: Plenum Publishing Corp., 1975:115-9.
- Guide for the Care and Use of Laboratory Animals, 8th edition. Washington (DC): National Academies Press (US), 2011.
- Dagrosa MA, Viaggi M, Rebagliati RJ, et al. Biodistribution of p-borophenylalanine (BPA) in dogs with spontaneous undifferentiated thyroid carcinoma (UTC). *Appl Radiat Isot* 2004;61:911-5.
- Dagrosa MA, Viaggi M, Kreimann E, et al. Selective uptake of p-borophenylalanine by undifferentiated thyroid carcinoma for boron neutron capture therapy. *Thyroid* 2002;12:7-12.
- Blachot J. Nuclear Data Sheets for A = 104. *Nuclear Data Sheets* 2007;108:2035-172.
- Blachot J. Nuclear Data Sheets for A = 116. *Nuclear Data Sheets* 2010;111:717-895.
- Blachot J. Nuclear Data Sheets for A = 114. *Nuclear Data Sheets* 2012;113: 515-714.
- Gürdal G. Nuclear Data Sheets for A = 110\*. *Nuclear Data Sheets* 2012;113:1315-561.
- Lee YS, Bullard DE, Zalutsky MR, et al. Therapeutic efficacy of antiangioma mesenchymal extracellular matrix

- 131I-radiolabeled murine monoclonal antibody in a human glioma xenograft model. *Cancer Res* 1988;48:559-66.
21. Shao Y, Gao Z, Marks PA, et al. Apoptotic and autophagic cell death induced by histone deacetylase inhibitors. *Proc Natl Acad Sci U S A* 2004;101:18030-5.
  22. Available online: <https://www-pub.iaea.org> > PDF > Pub1113\_scr1
  23. Dargosa MA, Thomasz L, Longhino J, et al. Optimization of boron neutron capture therapy for the treatment of undifferentiated thyroid cancer. *Int J Radiat Oncol Biol Phys* 2007;69:1059-66.
  24. Qiu L, Burgess A, Fairlie DP, et al. Histone deacetylase inhibitors trigger a G2 checkpoint in normal cells that is defective in tumor cells. *Mol Biol Cell* 2000;11:2069-83.
  25. Taddei A, Maison C, Roche D, et al. Reversible disruption of pericentric heterochromatin and centromere function by inhibiting deacetylases. *Nat Cell Biol* 2001;3:114-20.
  26. Dowling M, Voong K, Kim M, et al. Mitotic spindle checkpoint inactivation by richostatin a defines a mechanism for increasing cancer cell killing by microtubule-disrupting agents. *Cancer Biol Ther.* 2005; 4:197-206.
  27. Nome RV, Bratland A, Harman G, et al. Cell cycle checkpoint signaling involved in histone deacetylase inhibition and radiation-induced cell death. *Mol Cancer Ther* 2005;4:1231-8.
  28. Perona M, Rodríguez C, Carpano M, et al. Improvement of the boron neutron capture therapy (BNCT) by the previous administration of the histone deacetylase inhibitor sodium butyrate for the treatment of thyroid carcinoma. *Radiat Environ Biophys* 2013;52:363-73.
  29. Ito H, Daido S, Kanzawa T, et al. Radiation-induced autophagy is associated with LC3 and its inhibition sensitizes malignant glioma cells. *Int J Oncol* 2005;26:1401-10.
  30. Baumann M, Krause M, Hill R. Exploring the role of cancer stem cells in radioresistance. *Nat Rev Cancer* 2008;8:545-54.
  31. Peng L, Xiong Y, Wang R, et al. Identification of a subpopulation of long-term tumor-initiating cells in colon cancer. *Biosci Rep* 2020;40:BSR20200437.
  32. Biesiekierski A, Khurram M, Li Y, et al. 2-Material selection for medical devices, In: Wen C. editor. *Woodhead Publishing Series in Biomaterials, Metallic Biomaterials Processing and Medical Device Manufacturing*. Elsevier, 2020:31-94.
  33. Sun T, Li Y, Huang Y, et al. Targeting glioma stem cells enhances anti-tumor effect of boron neutron capture therapy. *Oncotarget* 2016;7:43095-108.
  34. Kondo N, Hikida M, Nakada M, et al. Glioma Stem-Like Cells Can Be Targeted in Boron Neutron Capture Therapy with Boronophenylalanine. *Cancers (Basel)* 2020;12:3040.

doi: 10.21037/tro-21-24

**Cite this article as:** Nieves SI, Carpano M, Boggio EF, Casal MR, Longhino JM, Dargosa MA. Experimental studies for the use of “beta enhancers” (BE) in the boron neutron capture therapy (BNCT) to optimize its application in the treatment of superficial tumors. *Ther Radiol Oncol* 2022;6:7.

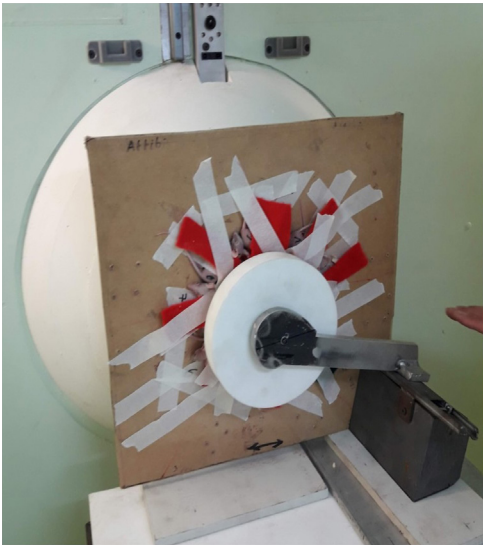


**Figure S1** Irradiation setup photo. Mice in groups of 8 animals were anesthetized and injected with BPA (350 mg/kg b.w) and positioned in the irradiation device in the reactor. The BE is placed over the tumor and attached with hypoallergenic tape. BPA, boronophenylalanine; BE, beta enhancers.

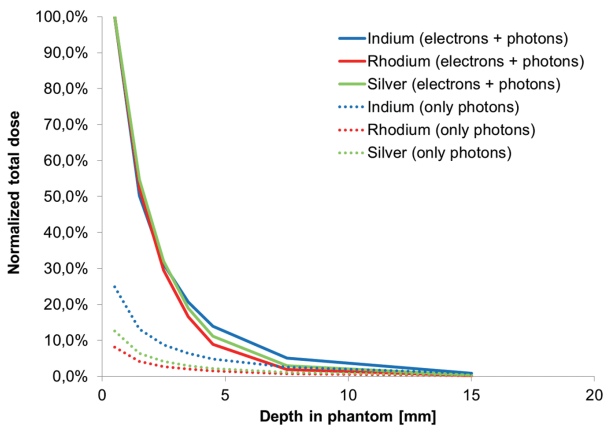


**Figure S2** Continued lines: BE in-depth total dose rates profiles comparison in a polystyrene phantom at the RA-6 BNCT beam (normalized to the first millimeter total dose of each BE). Dotted lines: photon dose component of each BE. BE, beta enhancers; BNCT, boron neutron capture therapy.